Interval Observer-Based Active Fault Tolerant Control for an Intensified Heat Exchanger/Reactor

Xue Han, Rim Rammal, Zetao Li, Michel Cabassud, Boutaib Dahhou

Interval Observer-Based Active Fault Tolerant Control for an Intensified Heat Exchanger/Reactor

Xue Han[1,2], Rim Rammal[2], Zetao Li[3,*], Michel Cabassud[4] and Boutaib Dahhou[2]

***Abstract*— The intensified heat exchanger/reactor systems, which combine the heat transfer and chemical reactions in one unit, became very popular and interesting in the chemical engineering field. However, to ensure the safety and maintain the performance of these systems, supervision, diagnosis, and fault tolerant control are highly demanded. In this paper, a fault tolerant control system, based on a bank of interval observers with a backstepping-based control law, is employed in a new intensified heat exchanger/reactor, in order to detect, isolate and recover all possible dynamic faults.**

I. INTRODUCTION

Inspired by the idea of process intensification (PI) [1][2][3] which can improve manufacturing, increase production capacity, and decrease energy consumption at the same time by reducing the size of equipment, a particular intensified heat-exchanger (HEX)/reactor has been developed in the LGC laboratory (Laboratoire de Génie Chimique). Thanks to the combination of reaction and heat exchange in one hybrid unit, the HEX reactor presents remarkable thermal and hydrodynamic performances [4]. However, different kinds of faults such as dynamic faults and sensor faults will cause a degradation of its performance. Therefore, advanced fault diagnosis (FD) and fault tolerant control (FTC) schemes are demanded to monitor the system states and interpret the system behaviors.

The FTC techniques are generally classified into two classes: passive FTC (PFTC) and active FTC (AFTC). See survey papers [5][6][7]. The PFTC uses a fixed controller, such as a robust controller, to deal with all types of faulty situations. It is less computationally complex, but its fault tolerant capability is limited. On the contrary, the AFTC consists of a fault detection, isolation, and identification (FDI) module that provides fault information and computes a reconfigurable controller in order to eliminate the fault. Compared to the PFTC, the AFTC is more flexible and it is capable of dealing with many types of faults [7].

For the AFTC systems, the FDI module has aroused the interest of many researchers. Various FDI methods have been developed in the past three decades, see [8][9][10]. Among these methods, the model-based methods have priority for the considered HEX reactor since its mathematical model has already been investigated in [11]. According to [12][13][14], the observer-based FDI approaches are proved to be reliable for the HEX reactor system. Besides, the interval observer-based FDI method proposed in [15][16] presents a quite fast speed of fault isolation and identification. In this paper, the interval observer-based FDI method is tested on the considered HEX reactor system, in order to detect, isolate, and identify dynamic faults.

In addition, in order to ensure the safety and performance of the HEX reactor, a fault reconfiguration strategy should be investigated along with the interval observer-based FDI method. In AFTC systems, fault reconfiguration can be performed by designing a new control law for the system using the fault information provided by the FDI module. In this paper, an AFTC system based on the backstepping technique is designed for the considered HEX reactor. Once the detail of the fault is obtained by the FDI module, the backstepping control law is redesigned to make the HEX reactor maintain its performance under the faulty case.

In this context, the paper is organized as follows: in Section II, the model of the HEX reactor system is presented and, in Section III, a control law is designed based on the backstepping theory. An AFTC system is given in Section IV, including an interval observer-based FDI module and the fault recovery procedure. Thereafter, simulation results are illustrated in Section V. Finally, Section VI concludes the paper and introduces some future work.

II. THE HEX REACTOR SYSTEM MODELING

Figure 1 presents the basic structure of the considered HEX reactor. It consists of three process plates (the red ones), four utility plates (the blue ones), and eight plate walls (the grey ones). Both the process plate and the utility plate have $2\,\mathrm{mm}$ square cross-section channels engraved into the steel. The plate walls are made of steel and act as the heat transfer media. Process fluid (the reactants, see $R1$ and $R2$ in Figure 1) is injected into the process channel, and the chemical reaction takes place here. Utility fluid (usually water) is injected into the utility channel to heat the process fluid or take away the generated reaction heat. The subscripts in and out represent the inlet and outlet fluid, respectively. According to the physical structure of the HEX reactor, the system is divided into 17 identical units, each unit contains 15 channels in total: 3 process channels, 4 utility channels

Research supported in part by the Agence Nationale de la Recherche (ANR), Project No. ANR-19-CE10-0007-04, France

*Corresponding author

[1]NORMANDIE UNIV, UNICAEN, ENSICAEN, LAC, Team IDO, 14000 Caen, France xue.han@unicaen.fr

[2]LAAS - CNRS, Université de Toulouse, CNRS, INSA, UPS, 31400 Toulouse, France rim.rammal@laas.fr (Rim Rammal), boutaib.dahhou@laas.fr (Boutaib Dahhou)

[3]Electrical Engineering College, Guizhou University, Guiyang 550025, China ztli@gzu.edu.cn

[4]LGC, Université de Toulouse, CNRS/INP/UPS, 31432 Toulouse, France michel.cabassud@ensiacet.fr

and 8 plate wall surface. Detailed information about the modeling process can be found in [11].

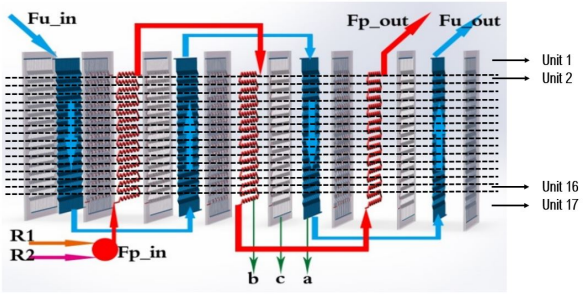

Fig. 1: *HEX reactor model, (a): utility plate, (b): process plate, (c) plate wall. Source [15].*

For simplicity, we consider the system with only 1 unit and without a chemical reaction in this paper. The model of the system is then represented by the following equations:

$$\begin{cases} \dot{T}_p = \dfrac{F_p}{V_p}(T_{p,in} - T_p) + \dfrac{h_p A_p}{\rho_p V_p C_{p,p}}(T_w - T_p) \\ \dot{T}_u = \dfrac{F_u}{V_u}(T_{u,in} - T_u) + \dfrac{h_u A_u}{\rho_u V_u C_{p,u}}(T_w - T_u) \\ \dot{T}_w = \dfrac{h_p A_p}{\rho_w V_w C_{p,w}}(T_p - T_w) + \dfrac{h_u A_u}{\rho_w V_w C_{p,w}}(T_u - T_w) \end{cases} \tag{1}$$

where $x = [T_p \quad T_u \quad T_w]^T$ is the state vector, $u = [F_p \quad F_u]^T$ is the input vector, and $y = [T_p \quad T_u]^T$ is the output vector. The variable T represents the temperature, F is the flow rate of the fluid. The subscript p, u and w represent the process channel, utility channel and the plate wall, respectively. ρ, V, h, A and C_p are density, volume, heat transfer coefficient, heat exchange area and specific heat of material, respectively. The physical parameters of the HEX reactor system are given in Table I.

TABLE I: Physical data of the HEX reactor

Parameter	Value	Units
V_p	2.68×10^{-5}	m^3
ρ_p, ρ_u	10^3	$\mathrm{kg \cdot m^{-3}}$
$C_{p,p}, C_{p,u}$	4.186×10^3	$\mathrm{J \cdot kg^{-1} \cdot K^{-1}}$
h_p	7.5975×10^3	$\mathrm{W \cdot m^2 \cdot K^{-1}}$
A_p	2.68×10^{-2}	m^2
V_u	1.141×10^{-4}	m^3
h_u	7.5833×10^2	$\mathrm{W \cdot m^2 \cdot K^{-1}}$
A_u	4.564×10^{-1}	m^2
V_w	1.355×10^{-3}	m^3
ρ_w	8×10^3	$\mathrm{kg \cdot m^{-3}}$
$C_{p,w}$	5×10^2	$\mathrm{J \cdot kg^{-1} \cdot K^{-1}}$

In the next section, a controller design of the system (1), based on the backstepping technique, is presented.

III. Backstepping Controller Design

The objective is to direct the output temperature of the process fluid T_p to the desired temperature $T_{p,d}$. To achieve this, a control law based on backstepping method is proposed for the considered HEX reactor system (1). In our case, the flow rate of utility fluid F_u is set as the only input to control the temperature of the process plate T_p, because the flow rate of the reactants F_p would generally have a fixed proportion to guarantee the efficiency of the chemical reaction.

The backstepping controller is designed as follow:

Step 1: Define the tracking error of the process temperature by $e_{T_p} = T_{p,d} - T_p$. Thus, from (1), the derivative of e_{T_p} is given by:

$$\begin{aligned} \dot{e}_{T_p} &= \dot{T}_{p,d} - \dot{T}_p \\ &= \dot{T}_{p,d} - \frac{F_p}{V_p}(T_{p,in} - T_p) - \frac{h_p A_p}{\rho_p V_p C_{p,p}}(T_w - T_p). \end{aligned} \tag{2}$$

Then, we define a positive definite Lyapunov function: $V_{T_p} = \frac{1}{2} e_{T_p}^2$, its derivative can be calculated:

$$\begin{aligned} \dot{V}_{T_p} &= e_{T_p} \dot{e}_{T_p} \\ &= e_{T_p}\Big(\dot{T}_{p,d} - \frac{F_p}{V_p}(T_{p,in} - T_p) - \frac{h_p A_p}{\rho_p V_p C_{p,p}}(T_w - T_p)\Big). \end{aligned} \tag{3}$$

To ensure the stability of the tracking error system e_{T_p}, i.e. make $\dot{V}_{T_p}$ be negative definite, the temperature of the plate wall T_w is chosen as the first virtual element of control with a desired value of $T_{w,d}$:

$$T_{w,d} = \frac{\rho_p V_p C_{p,p}}{h_p A_p}\left[\dot{T}_{p,d} + k_1 e_{T_p} - \frac{F_p}{V_p}(T_{p,in} - T_p)\right] + T_p \tag{4}$$

where k_1 is a positive design parameter. By setting $T_w = T_{w,d}$ in (3), we get $\dot{V}_{T_p} = -k_1 e_{T_p}^2 \leq 0$.

Step 2: Similarly, we define the tracking error $e_{T_w} = T_{w,d} - T_w$ and calculate its derivative: $\dot{e}_{T_w} = \dot{T}_{w,d} - \dot{T}_w$.

Then, we define a positive definite Lyapunov function: $V_{T_w} = \frac{1}{2} e_{T_p}^2 + \frac{1}{2} e_{T_w}^2 = V_{T_p} + \frac{1}{2} e_{T_w}^2$, and calculate its derivative:

$$\dot{V}_{T_w} = \dot{V}_{T_p} + e_{T_w} \dot{e}_{T_w}. \tag{5}$$

In order to make $\dot{V}_{T_w}$ be negative definite, the temperature of utility fluid T_u is chosen as the second element of virtual control with a desired value of $T_{u,d}$:

$$\begin{aligned} T_{u,d} = \frac{\rho_w V_w C_{p,w}}{h_u A_u}\Bigg[& \frac{h_p A_p}{\rho_p V_p C_{p,p}} e_{T_p} \\ & + \frac{\rho_p V_p C_{p,p}}{h_p A_p}(\ddot{T}_{p,d} + k_1 \dot{e}_{T_p} + \frac{F_p}{V_p}\dot{T}_p) + \dot{T}_p \\ & - \frac{h_p A_p}{\rho_w V_w C_{p,w}}(T_p - T_w) + k_2 e_{T_w}\Bigg] + T_w \end{aligned} \tag{6}$$

where k_2 is a positive parameter. By setting $T_u = T_{u,d}$ in (5), we get: $\dot{V}_{T_w} = -k_1 e_{T_p}^2 - k_2 e_{T_w}^2 \leq 0$.

Step 3: Define the tracking error of the utility temperature $e_{T_u} = T_{u,d} - T_u$. Its derivative is given by: $\dot{e}_{T_u} = \dot{T}_{u,d} - \dot{T}_u$.

In order to make the tracking error system e_{T_u} converge to zero, a third positive definite Lyapunov function is defined $V_{T_u} = \frac{1}{2} e_{T_p}^2 + \frac{1}{2} e_{T_w}^2 + \frac{1}{2} e_{T_u}^2 = V_{T_w} + \frac{1}{2} e_{T_u}^2$ with a derivative given by:

$$\dot{V}_{T_u} = \dot{V}_{T_w} + e_{T_u} \dot{e}_{T_u}. \tag{7}$$

Finally, we get the expression of the control law F_u:

$$\begin{aligned} F_u =& \frac{V_u}{T_{u,in}-T_u}\Big\{\frac{h_u A_u}{\rho_w V_w C_{p,w}} e_{T_w} + \frac{\rho_w V_w C_{p,w}}{h_u A_u} \\ & \Big[\frac{h_p A_p}{\rho_p V_p C_{p,p}}\dot{e}_{T_p} + \frac{\rho_p V_p C_{p,p}}{h_p A_p}(\dddot{T}_{pd} + k_1 \ddot{e}_{T_p} + \frac{F_p}{V_p}\ddot{T}_p) \\ & + \ddot{T}_p - \frac{h_p A_p}{\rho_w V_w C_{p,w}}(\dot{T}_p - \dot{T}_w) + k_2 \dot{e}_{T_w}\Big] \\ & + \frac{h_p A_p}{\rho_w V_w C_{p,w}}(T_p - T_w) + \frac{h_u A_u}{\rho_w V_w C_{p,w}}(T_u - T_w) \\ & - \frac{h_u A_u}{\rho_u V_u C_{p,u}}(T_w - T_u) + k_3 e_{T_u}\Big\} \end{aligned} \tag{8}$$

where k_3 is a positive design parameter. It can ensure the stability of e_{T_u}, i.e. make $\dot{V}_{T_u}$ be negative definite: $\dot{V}_{T_u} = -k_1 e_{T_p}^2 - k_2 e_{T_w}^2 - k_3 e_{T_u}^2 \leq 0$. Moreover, the gains k_1, k_2, and k_3 are chosen with a goal to obtain a satisfactory dynamic of the control law.

As mentioned above, the HEX reactor is highly intensified, so it cannot be opened to clean after the assembly. Thus, the fouling caused by the accumulation of products may directly degrade the behavior of heat exchange. Besides, the inlet fluid temperature change caused by malfunction of the thermocouples, is also one of the typical dynamic fault for the HEX reactor. To maintain the performance of the pilot in presence of a dynamic fault, an interval observer-based AFTC method is presented in the next section.

IV. Interval observer-based AFTC

Generally, an AFTC consists of two steps, FDI at the first step and controller redesign at the second one to eliminate the influence of the fault. In this section, an AFTC scheme based on interval observers is presented.

A. Observer formulation and fault diagnosis

Consider the following nonlinear system:

$$\begin{cases} \dot{x} = f(x, \theta, u) \\ y = Cx \end{cases} \tag{9}$$

where $x \in \mathcal{R}^n$ is the state vector, $\theta \in \mathcal{R}^m$ is the possible faulty parameter vector, $y \in \mathcal{R}^q$ is the output vector, $C \in \mathcal{R}^{q\times n}$ is the output matrix. $f(x, \theta, u)$ is a nonlinear function, and its first partial derivatives on x and θ are continuous, bounded, Lipschitz in x and θ. The nominal value of the parameter vector θ is denoted by θ^0 and is known.

The authors in [15][16] define the parameter fault as a vector given by: $f_p = \theta^f - \theta^0$, which will cause a great deviation between the faulty system $\dot{x} = f(x, \theta^f, u)$ and its nominal model $\dot{x} = f(x, \theta^0, u)$. θ^f indicates the faulty parameter vector.

In order to detect, isolate and identify the faulty parameter, we use a FDI method based on interval observers[15][16], the observers are constructed by the divided intervals of the possible faulty parameter. Then, all the intervals are checked to figure out whether or not one of them contains the faulty parameter value. Thus, the fault is isolated and estimated.

To design a bank of interval observers for the dynamic system (9), the practical domain of the possible faulty parameters is firstly divided into several intervals. The interval diving rule can base on the specific value change or the percentage change of the nominal value. For celerity, we take the ith interval of the jth parametere $\theta^{(j)}$ as an example, the interval bounds are denoted by $\theta^{(i,j)}$ and $\theta^{(i+1,j)}$.

Then, the isolation observers corresponding to each interval bound are given below:

$$\begin{cases} \dot{\hat{x}}^{(i,j)} = f(\hat{x}^{(i,j)}, \theta^{ob(i,j)}(t), \theta^{ob(i,l)}(t), u) + H(\hat{y}^{(i,j)} - y) \\ \hat{y}^{(i,j)} = C\hat{x}^{(i,j)} \\ e_y^{(i,j)} = \hat{y}^{(i,j)} - y \end{cases} \tag{10}$$

$$\begin{cases} \dot{\hat{x}}^{(i+1,j)} = f(\hat{x}^{(i+1,j)}, \theta^{ob(i+1,j)}(t), \theta^{ob(i+1,l)}(t), u) \\ \qquad\qquad + H(\hat{y}^{(i+1,j)} - y) \\ \hat{y}^{(i+1,j)} = C\hat{x}^{(i+1,j)} \\ e_y^{(i+1,j)} = \hat{y}^{(i+1,j)} - y \end{cases} \tag{11}$$

where

$$\theta^{ob(i,j)}(t) = \begin{cases} \theta^{0(j)}, t < t_f, \\ \theta^{(i,j)}, t \geq t_f, \end{cases} \quad \theta^{ob(i+1,j)}(t) = \begin{cases} \theta^{0(j)}, t < t_f, \\ \theta^{(i+1,j)}, t \geq t_f, \end{cases}$$

$$\theta^{ob(i,l)}(t) = \theta^{ob(i+1,l)}(t) = \theta^{0(l)}, \forall t, \quad l \neq j$$

As presented in (10) and (11), each bound of parameter intervals is used as a parameter of the isolation observer. For one parameter with n intervals in series, there are $(n+1)$ bounds, so, $(n+1)$ isolation observers are constructed.

To detect the occurrence of a fault, we only need to calculate the residual of a special observer that uses the nominal parameter value. Suppose that the kth observer is the particular one, then the residual is defined as:

$$r_k = \|\hat{y}^{(k)} - y\|, \quad k \in 1, \ldots, m. \tag{12}$$

where $\hat{y}^{(k)}$ and y represent the output vector of the kth observer and of the system, respectively. If, at some point of the system operation, the residuals become different from zero, then a fault in the open-loop system is detected.

Remark 1: In the closed-loop system, the residual can be easily affected by the input signal change, which makes it difficult to identify the reason for the residual change. In this paper, we suppose that all the actuators are fault-free, which eliminates the possibility that the affected residual is caused by an actuator fault.

In order to identify the reason for residual change, input variation caused by the controller adjustment or a fault in the system parameter, auxiliary residual Dr_k is introduced:

$$Dr_k = \frac{d\|\hat{y}^{(k)} - y\|}{dt} \tag{13}$$

The auxiliary residual is used to evaluate the stability of the original residuals r_k. Therefore, we check the value of the original residual r_k and auxiliary residual Dr_k at the first step, if they all leave zero then a state change is detected. Second, when the auxiliary residual Dr_k goes back to zero,

i.e. the original residual r_k is stable, we evaluate its value. If r_k goes back to zero, then the change is caused by an input adjustment. However, if r_k stays at a nonzero value, then the change indicates the occurrence of a fault.

Once the fault is detected, we calculate the index of each interval to isolate the fault:

$$v^{(i,j)} = sgn(e_y^{(i,j)})sgn(e_y^{(i+1,j)}) \tag{14}$$

$v^{(i,j)} = 1$ indicates that this interval does not contain the faulty parameter value. In the contrast, $v^{(i,j)} = -1$ indicates that the faulty parameter value is located in this interval.

If the ith interval of jth parameter contains the faulty parameter, the fault value can be obtained by the following:

$$\hat{\theta}^{f(j)} = \frac{1}{2}(\theta^{(i,j)} + \theta^{(i+1,j)}) \tag{15}$$

This estimation of the faulty parameter value do not rely on classic parameter identification methods but rely on the proposed fault isolation method. And the fault is identified the moment the fault is isolated. Therefore, the time of FDI depends on the convergence time of the original residual.

B. Fault recovery

As long as the fault on the jth parameter is diagnosed, we proceed to the calculation of the faulty value $\hat{f}_p^{(j)}$, using the parameter estimation in (15):

$$\hat{f}_p^{(j)} = \hat{\theta}^{f(j)} - \theta^{0(j)}. \tag{16}$$

In order to recover the dynamic fault, the estimated faulty value $\hat{f}_p^{(j)}$ is used to redesign the control signal F_u given by (8), by replacing the faulty parameter $\theta^{f(j)}$ by $\theta^{0(j)} + \hat{f}_p^{(j)}$.

V. Simulation Results

A case study is developed to test the effectiveness of the proposed AFTC method. The objective is to make the measured process fluid temperature T_p follows the desired value $T_{p,d}$ in presence of dynamic faults. In the simulation, the following data obtained from real experiment [4] is used: $F_p = 10\,\mathrm{L}\cdot\mathrm{h}^{-1}$, $T_{p,in} = 77\,^\circ\mathrm{C}$, $F_u = 62.2\,\mathrm{L}\cdot\mathrm{h}^{-1}$, $T_{u,in} = 15.6\,^\circ\mathrm{C}$. Due to the physical limitation of the pump, the flow rate of both fluids ranges from 0 to $150\,\mathrm{L}\cdot\mathrm{h}^{-1}$. The initial temperatures of process channel, utility channel and plate wall are $[T_p \quad T_u \quad T_w]^T = [77 \quad 15.6 \quad 15.6]^T$.

In the fault free case, the measured temperature of the process fluid T_p and the control input F_u are presented in Figure 2. The desired temperature $T_{p,d}$ is firstly settled at $27\,^\circ\mathrm{C}$ and then resettled at $25^\circ\mathrm{C}$ at $t = 400\,\mathrm{s}$. A filter is applied to the reference temperature in order to get a smoothing input signal. According to the designed control law and physical restriction of the pumps, the flow rate of utility fluid F_u is set either to the minimum value $0\,\mathrm{L}\cdot\mathrm{h}^{-1}$ or the maximum value $150\,\mathrm{L}\cdot\mathrm{h}^{-1}$ to track the desired temperature as fast as possible during the transition period.

The dynamic faults considered in this paper are the decrease of the heat transfer coefficient between the process plate and the plate wall h_p caused by the fouling in the process channels, and the inlet temperature change of the process fluid $T_{p,in}$ caused by environment temperature change or malfunction of the thermocouple. Their nominal values are $\begin{bmatrix} h_p^0 & T_{p,in}^0 \end{bmatrix}^T = \begin{bmatrix} 7.5975 \times 10^3 & 77 \end{bmatrix}^T$. To start, both parameters are divided into five intervals with six bounds. Therefore, twelve isolation observers are constructed. The bounds of each interval are given in Table II and Table III. The interval diving of h_p is based on the percentages of its nominal value h_p^0, while the interval partition of $T_{p,in}$ is related to the specific values around its nominal value $T_{p,in}^0$.

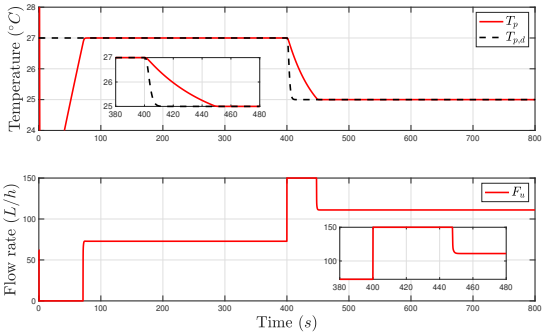

Fig. 2: *Measured process fluid temperature T_p and utility fluid flow rate F_u in the fault free case.*

TABLE II: The value of interval bounds for h_p

No. of interval	1	2	3	4	5
$h_p^{(a)}$	100%	90%	80%	70%	60%
$h_p^{(b)}$	90%	80%	70%	60%	50%

TABLE III: The value of interval bounds for $T_{p,in}$

No. of interval	1	2	3	4	5
$T_{p,in}^{(a)}$	81	79	77	75	73
$T_{p,in}^{(b)}$	79	77	75	73	71

A. Dynamic fault on h_p

At $t_f = 200\,\mathrm{s}$, the heat transfer coefficient h_p decreases 15% of its nominal value, i.e. $f_p^{(h_p)} = -1.393 \times 10^3\ \mathrm{W}\cdot\mathrm{m}^2\cdot\mathrm{K}^{-1}$. Then, the heat transfer coefficient in the faulty case becomes $h_p^f = h_p^0 + f_p^{(h_p)} = 6.4852\times10^3\ \mathrm{W}\cdot\mathrm{m}^2\cdot\mathrm{K}^{-1}$.

According to Table II, the first isolation observer is the special one that uses the nominal value h_p^0. Its original residual r_1 and the auxiliary residual Dr_1, used for FDI, are represented in Figure 3. At about $t = 72\,\mathrm{s}$, the original residual r_1 and the auxiliary residual Dr_1 change. When the auxiliary residual goes back to zero, i.e. the original residual is stable, the original residual also goes back to zero. Then, this means that the change is caused by a simple change of the control signal and not by a fault.

At $200\,\mathrm{s}$, both original and auxiliary residual change. When Dr_1 goes back to zero, r_1 stays at a nonzero value. Therefore, a fault is detected in the system.

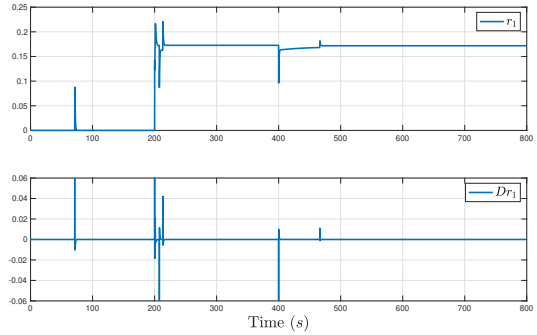

Fig. 3: *Original residual and auxiliary residual of the special observer:* h_p *is faulty at* 200 s.

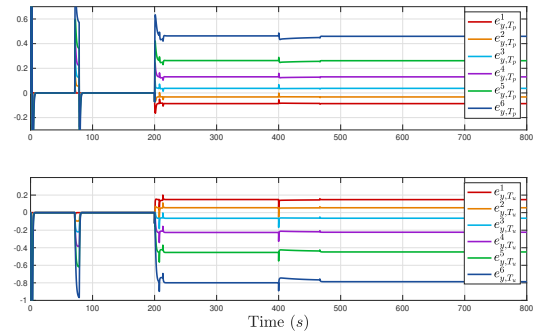

Fig. 4: Output error vector e_y correspond to intervals of h_p when dynamic h_p is faulty at $200s$

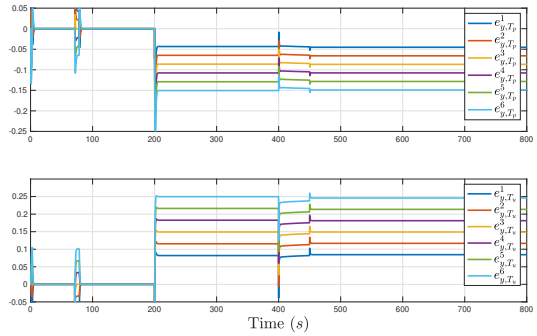

Fig. 5: Output error vector e_y correspond to intervals of $T_{p,in}$ when dynamic h_p is faulty at $200s$

To isolate the fault, we check the performance of the output error vector $e_y = \begin{bmatrix} e_{y,T_p} & e_{y,T_u} \end{bmatrix}^T$. Figure 4 shows the output error vector e_y between the interval observers corresponding to h_p and the real system, while Figure 5 presents the e_y between the observers corresponding to $T_{p,in}$ and the real system.

In Figure 4, the zero is sandwiched by the second and the third output error e_y^2 and e_y^3. That is to say that the isolation index $v^{(2,h_p)} = sgn(e_y^{(2,h_p)})sgn(e_y^{(3,h_p)}) = -1$, while others are equal to one. On the other hand, the isolation indexes $v^{(T_{p,in})}$ corresponding to the parameter $T_{p,in}$ are all equal to one, because the output error e_y is located in the same side of zero in Figure 5. According to the isolation rule, the fault is isolated in the second interval of h_p. The value of the fault is therefore estimated immediately:

$$\hat{h}_p^f = \frac{1}{2}(h_p^{(2)} + h_p^{(3)}) = \frac{1}{2}(90\%h_p^0 + 80\%h_p^0) = 85\%h_p^0 \tag{17}$$

Finally, the fault information is used to redesign the controller. Figure 6 represents the process temperature T_p under two different situations: when the AFTC method is applied and when it is not. It is clear that the process temperature T_p cannot follow the desired value $T_{p,d}$ without the AFTC strategy. On the contrary, the fault on h_p is recovered when the AFTC method is applied, and the system continues to operate safely.

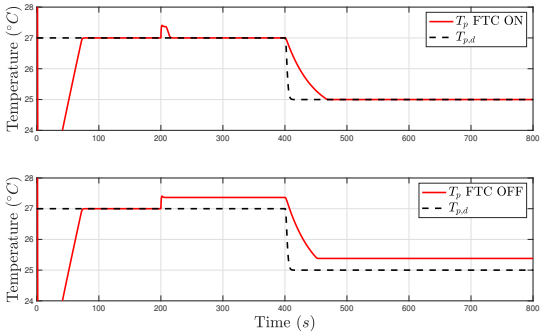

Fig. 6: *Temperature* T_p *under different cases:* h_p *is faulty at* 200 s.

B. Dynamic fault on $T_{p,in}$

In the second case, a fault $f_p^{(T_{p,in})} = -5\,^\circ$C is added to the inlet temperature of process fluid at $t_f = 200$ s. Then, $T_{p,in}^f = T_{p,in}^0 + f_p^{(T_{p,in})} = 73^\circ$C. From Table III, the third observer is the particular one because it uses the nominal value $T_{p,in}^0 = 77^\circ$C. The residuals are shown in Figure 7. After $t_f = 200$ s, and when the original residual r_3 is stable, it stays at a non zero value. Then, the fault is detected.

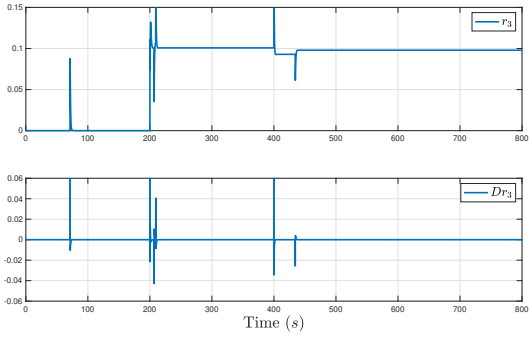

Fig. 7: *Original residual and auxiliary residual of the special observer:* $T_{p,in}$ *is faulty at* 200 s.

With the help of the output error vector e_y shown in Figure 8 and Figure 9, we can easily calculate the isolation index and find the special one: $v^{(5,T_{p,in})} = sgn(e_y^{(5,T_{p,in})})sgn(e_y^{(6,T_{p,in})}) = -1$, i.e. the fault is located in the fifth interval of $T_{p,in}$.

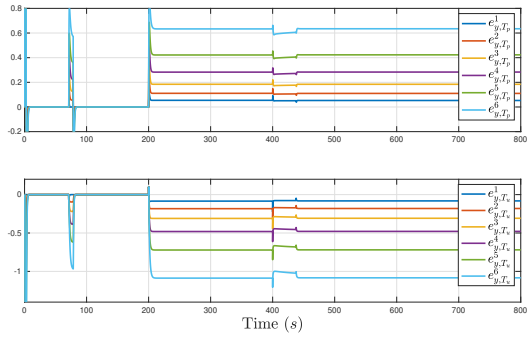

Fig. 8: Output error vector e_y correspond to intervals of h_p when dynamic $T_{p,in}$ is faulty at $200s$

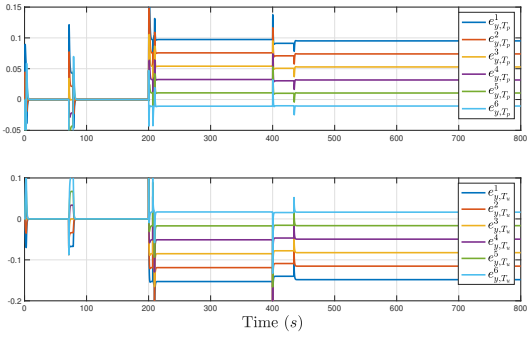

Fig. 9: Output error vector e_y correspond to intervals of $T_{p,in}$ when dynamic $T_{p,in}$ is faulty at $200s$

Therefore, the fault is estimated:

$$\hat{T}^f_{p,in} = \frac{1}{2}(T^{(5)}_{p,in} + T^{(6)}_{p,in}) = \frac{1}{2}(71 + 73) = 72 \qquad (18)$$

and is used for the controller redesign procedure.

Figure 10 represents the performance of the system with and without the application of the AFTC strategy. Obviously, the AFTC scheme eliminates the effect of the fault.

VI. CONCLUSION

In this paper, an interval observer-based AFTC system is proposed to an intensified HEX reactor. With the help of the interval observer construction, the fault is detected, isolated and identified. The backstepping based control law proposed in this paper is then redesigned by using the estimated fault information. The effectiveness of the interval observer-based AFTC method is validated by simulations. In the future, experiments will be conducted to verify the performance of the proposed AFTC strategy, this method will also be applied to recover the faults on the sensors and the actuators.

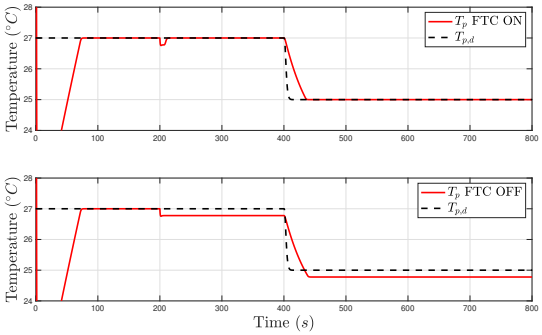

Fig. 10: *Temperature T_p under different cases: $T_{p,in}$ is faulty at* 200 s.

REFERENCES

[1] Stankiewicz, Andrzej I., and Jacob A. Moulijn. "Process intensification: transforming chemical engineering." Chemical engineering progress 96, no. 1 (2000): 22-34.

[2] Etchells, J. C. "Process intensification: Safety pros and cons." Process Safety and Environmental Protection 83, no. 2 (2005): 85-89.

[3] Green, A., B. Johnson, and A. John. "Process intensification magnifies profits." Chemical engineering (New York, NY) 106, no. 13 (1999): 66-73.

[4] Theron, Félicie, Zoé Anxionnaz-Minvielle, Michel Cabassud, Christophe Gourdon, and Patrice Tochon. "Characterization of the performances of an innovative heat-exchanger/reactor." Chemical Engineering and Processing: Process Intensification 82 (2014): 30-41.

[5] Gao, Zhiwei, Carlo Cecati, and Steven X. Ding. "A survey of fault diagnosis and fault-tolerant techniques—Part I: Fault diagnosis with model-based and signal-based approaches." IEEE transactions on industrial electronics 62.6 (2015): 3757-3767.

[6] Gao, Zhiwei, Carlo Cecati, and Steven X. Ding. "A survey of fault diagnosis and fault-tolerant techniques—Part II: Fault diagnosis with knowledge-based and hybrid/active approaches." IEEE Transactions on Industrial Electronics 62.6 (2015): 3768-3774.

[7] Amin, Arslan Ahmed, and Khalid Mahmood Hasan. "A review of fault tolerant control systems: advancements and applications." Measurement 143 (2019): 58-68.

[8] Punčochář, Ivo, and Jan Škach. "A survey of active fault diagnosis methods." IFAC-PapersOnLine 51.24 (2018): 1091-1098.

[9] Zhou, Yimin, Guoqing Xu, and Qi Zhang. "Overview of fault detection and identification for non-linear dynamic systems." In 2014 IEEE International Conference on Information and Automation (ICIA), pp. 1040-1045. IEEE, 2014.

[10] Thirumarimurugan, M., N. Bagyalakshmi, and P. Paarkavi. "Comparison of fault detection and isolation methods: A review." In 2016 10th International Conference on Intelligent Systems and Control (ISCO), pp. 1-6. IEEE, 2016.

[11] Menglin He, Zetao Li, Xue Han, Michel Cabassud, and Boutaib Dahhou. "Development of a Numerical Model for a Compact Intensified Heat-Exchanger/Reactor." Processes 7, no. 7 (2019): 454.

[12] Mei Zhang, Zetao Li, Michel Cabassud, and Boutaib Dahhou. "An integrated FDD approach for an intensified HEX/Reactor." Journal of Control Science and Engineering 2018 (2018).

[13] Mei Zhang, Boutaib Dahhou, Qinmu Wu, and Zetao Li. "Observer Based Multi-Level Fault Reconstruction for Interconnected Systems." Entropy 23.9 (2021): 1102.

[14] Zetao Li, Boutaib Dahhou, Mei Zhang, and Michel Cabassud. "Actuator gain fault diagnosis for heat-exchanger/reactor." 2015 Chinese Automation Congress (CAC). IEEE, 2015.

[15] Zetao Li, and Boutaieb Dahhou. "A new fault isolation and identification method for nonlinear dynamic systems: Application to a fermentation process." Applied Mathematical Modelling 32.12 (2008): 2806-2830.

[16] Zetao Li, and Boutaieb Dahhou. "Fault isolation for nonlinear dynamic systems based on parameter intervals." International Journal of Systems Science 38.7 (2007): 531-547.